Organic & Biomolecular Chemistry

PAPER

View Article Online
View Journal | View Issue

Cite this: *Org. Biomol. Chem.*, 2014, **12**, 6684

Synthesis and evaluation of antineurotoxicity properties of an amyloid-β peptide targeting ligand containing a triamino acid†

Dmytro Honcharenko,*[a] Partha Pratim Bose,[a] Jyotirmoy Maity,[a] Firoz Roshan Kurudenkandy,[b] Alok Juneja,[a] Erik Flöistrup,[a] Henrik Biverstål,[c] Jan Johansson,[c] Lennart Nilsson,[a] André Fisahn[b] and Roger Strömberg*[a]

Received 9th May 2014,
Accepted 27th June 2014

DOI: 10.1039/c4ob00959b

www.rsc.org/obc

Peptide-like compounds containing an arginine have been shown to bind and stabilize the central helix of the Alzheimer's disease related amyloid-β peptide (Aβ) in an α-helical conformation, thereby delaying its aggregation into cytotoxic species. Here we study a novel Aβ targeting ligand AEDabDab containing the triamino acid, N^{γ}-(2-aminoethyl)-2,4-diaminobutanoic (AEDab) acid. The new AEDab triamino acid carries an extra positive charge in the side chain and is designed to be incorporated into a ligand AEDabDab where the AEDab replaces an arginine moiety in a previously developed ligand Pep1b. This is done in order to increase the Aβ–ligand interaction, and molecular dynamics (MD) simulation of the stability of the Aβ central helix in the presence of the AEDabDab ligand shows further stabilization of the helical conformation of Aβ compared to the previously reported Pep1b as well as compared to the AEOrnDab ligand containing an N^{δ}-(2-aminoethyl)-2,5-diaminopentanoic acid unit which has an additional methylene group. To evaluate the effect of the AEDabDab ligand on the Aβ neurotoxicity the AEDab triamino acid building block is synthesized by reductive alkylation of N-protected-glycinal with α-amino-protected diaminobutanoic acid, and the Aβ targeting ligand AEDabDab is prepared by solid-phase synthesis starting with attachment of glutarate to the Wang support. Replacement of the arginine residue by the AEDab triamino acid resulted in an improved capability of the ligand to prevent the $A\beta_{1-42}$ induced reduction of gamma (γ) oscillations in hippocampal slice preparation.

Introduction

A number of diseases are associated with misfolding and aggregation of proteins or peptides into structures known as amyloid fibrils. Such protein misfolding diseases include for example Alzheimer's disease (AD), type II diabetes, Parkinson's and Creutzfeldt–Jakob's diseases.[1,2]

One of the hallmarks of AD is cerebral extracellular deposits, called plaques, which are mainly composed of amyloid fibrils formed from the amyloid-β peptide (Aβ).[3] Aβ is an amphiphilic peptide of mainly 40- or 42-residues produced by enzymatic cleavages from an integral membrane protein, the amyloid precursor protein (APP).[4,5] Formation of such fibrils through aggregation of Aβ in a β-strand-like conformation is thought to be a major part of the cause of AD.[6,7] However, more and more findings point to the toxic nature of prefibrillar soluble aggregates, such as soluble Aβ oligomers, produced early in the aggregation pathway.[8–10] Initially, when generated from APP, Aβ harbours a discordant α-helix with residues that have a high propensity for β-strand formation.[11] This region of Aβ (residue 16–23) serves as a binding sequence during its polymerization,[12,13] and recent structural models for amyloid fibrils[14,15] support the fact that the residues 17–24 in the discordant helix of $A\beta_{1-42}$ are essential for fibril formation.[16] Inhibition of Aβ aggregation could prevent the occurrence or progression of AD. Various strategies were developed[17] to achieve this including targeting of Aβ in an elongated, β-strand-like conformation with a range of small organic molecules or peptide-based inhibitors.[18] The disadvantages of these strategies are the lack of specificity and potential

[a]*Department of Biosciences and Nutrition, Karolinska Institutet, S-14183 Huddinge, Sweden. E-mail: Roger.Stromberg@ki.se, Dmytro.Honcharenko@ki.se; Fax: +46-8-52481025; Tel: +46-8-52481024*
[b]*Neuronal Oscillations Laboratory, Division for Neurogeriatrics, KI-Alzheimer Disease Research Center, Department of Neurobiology, Care Sciences and Society, Karolinska Institute, Stockholm, Sweden 14186 Huddinge, Sweden*
[c]*KI-Alzheimer Disease Research Center, Department of Neurobiology, Care Sciences and Society, Karolinska Institute, 14186 Huddinge, Sweden*

†Electronic supplementary information (ESI) available: ^{1}H spectra of compounds **3–6**, **11**, **12**, ^{13}C APT NMR spectra of compounds **3–6**, ESI-TOF MS spectra of compounds **11** and **12**, HPLC chromatograms of crude compounds **11** and **12**, and ^{1}H–^{1}H COSY spectra of compounds **11** and **12**. See DOI: 10.1039/c4ob00959b

accumulation of cytotoxic soluble, non-fibrillar Aβ aggregates.[19]

We have reported on inhibition of Aβ aggregation *in vitro* by targeting the discordant region of the Aβ central helix with ligands stabilizing its α-helical conformation, which is similar to the native structure in membrane embedded APP.[20] Oral administration of these inhibitors in *Drosophila melanogaster* expressing human $A\beta_{1-42}$ in the central nervous system[21] resulted in a prolonged lifespan, a decrease of locomotor dysfunction and reduction of neuronal damage. The ligands also partially prevented Aβ-induced reduction of γ oscillations in hippocampal slices, an activity which is important for memory and cognition and is reduced in Alzheimer's patients.[22] Stabilization of the central α-helix in Aβ appears to counteract aggregation and formation of toxic assemblies. Additional support for this concept comes from recent molecular dynamics simulations that also uncover details of the mechanism of unfolding of the Aβ central helix[23] as well as retardation of the folding in the presence of ligands designed to interact with the native helical conformation.[24,25] In view of these observations we are developing a new generation of ligands[26] with the aim of increasing their interaction with the helical Aβ. The present study describes synthesis and evaluation of the novel Aβ targeting ligand AEDabDab carrying a new positively charged triamino acid, N^{γ}-(2-aminoethyl)-2,4-diaminobutanoic acid (AEDab). The influence of the AEDab triamino acid on the interaction between Aβ peptides and new ligands is studied by molecular dynamics (MD) and the prevention of Aβ toxicity by γ oscillation experiments in hippocampal slice preparation.

Results and discussion

Design of ligands containing triamino acids

The α-helical form of the central region (residues 13–26; H^{13}HQKLVFFAEDVGS[26]) of Aβ can be a target for stabilizing ligands. The previously developed Aβ targeting peptide-like ligand Pep1b[20] was intended to interact with this region of Aβ through charge–charge interactions and hydrophobic contacts (Fig. 1A). The negatively charged residues Glu22 and Asp23 in the C-terminal end of Aβ were targeted by the arginine residue of Pep1b carrying two positive charges. We suspected that the replacement of the arginine residue in a new ligand by a moiety with an extra positive charge could provide additional interactions with the negatively charged region of Aβ and improve binding of the ligand in general. The previously reported triamino acid, 4-azalysine,[27,28] was a bit short, so to investigate the above concept we replaced the arginine residue by the new triamino acids AEDab and AEOrn in the corresponding AEDabDab (Fig. 1B) and AEOrnDab (Fig. 1C) ligands. The complexes of these molecules with $A\beta_{13-26}$ were then studied using MD simulation. We chose to look at AEDab and AEOrn triamino acids because of their structural similarity to arginine and to allow direct comparison with the previously reported Pep1b. The replacement of the arginine residue by these triamino acids with side chains that at physiological pH should be largely doubly protonated should lead to an additional positive charge in the ligand while keeping approximately the same overall molecular size and distance between charges in the side chain and the α position of the amino acid.

Modeling studies on Aβ

In our earlier reports[23–25] we performed simulation studies on $A\beta_{13-26}$ using explicit solvent (ES) and various implicit solvent (IS) models to capture the unfolding of $A\beta_{13-26}$ and its stabilization by ligands. The results from the IS model GMBV II,[29] an analytical Generalized Born model using molecular volume,[30] are found to be in agreement with recently performed ES simulation studies.[24] Therefore, GBMV II is used in the present study to compare the effect of AEDabDab and AEOrnDab ligands with that of the previously reported Pep1b[20] on the stability of the Aβ central helix in molecular dynamics of a defined length (100 ns) using the same stability criteria as in the earlier IS simulation study.[25]

Effects of ligands on the stability of $A\beta_{13-26}$

The results from MD simulation show trends of $A\beta_{13-26}$ unfolding and an increase in the stability of the helix in the presence of the ligands. $A\beta_{13-26}$ is unfolded in the absence of either of the ligands with average RMSD of conformers of 3.9 Å and average number of α-helical backbone hydrogen bonds (αHBs) of 1.6 (Table 1). All ligands enhance the stability of $A\beta_{13-26}$ in a helical state as is seen in the average values of αHBs count and backbone RMSDs (Table 1). The AEDabDab performed somewhat better than Pep1b and showed significantly larger average number of polar contacts with $A\beta_{13-26}$ compared to AEOrnDab (Table 1). This suggests that the extra methylene group in AEOrnDab compared to AEDabDab and Pep1b brings some modulation in the interaction between ligands and $A\beta_{13-26}$ and leads to decrease of polar contacts and increase of non-polar contacts with $A\beta_{13-26}$ (Table 1).

Analysis of distribution of the backbone heavy atoms RMSD and number of αHBs of $A\beta_{13-26}$ in the presence of AEDabDab shows similar results as in the presence of Pep1b with RMSD < 2 Å (Fig. 2A) and αHBs 3–6 (Fig. 2B). However, AEDabDab displayed more polar and non-polar contacts with $A\beta_{13-26}$ as compared to Pep1b (Fig. 3). This can be related to the fact that an extra basic functional group in AEDabDab gives additional polar contacts with acidic residues of $A\beta_{13-26}$ but also that the ethylene group between the two amines in the side chain gives some additional non-polar contacts with the adjacent phenylalanine (Phe19). A secondary effect could be that the centrally placed indole moiety in the ligand is kept less flexible and gives additional non-polar contact with the Phe20. The indication from the molecular dynamics is then that the AEDabDab ligand is the most promising and it could give some improvement over Pep1b with respect to interaction with and prevention of toxicity of the Aβ peptide. Thus, we decided to prepare the AEDabDab ligand and test it in *in vitro* experiments as a model Aβ targeting ligand that carries the AEDab triamino acid.

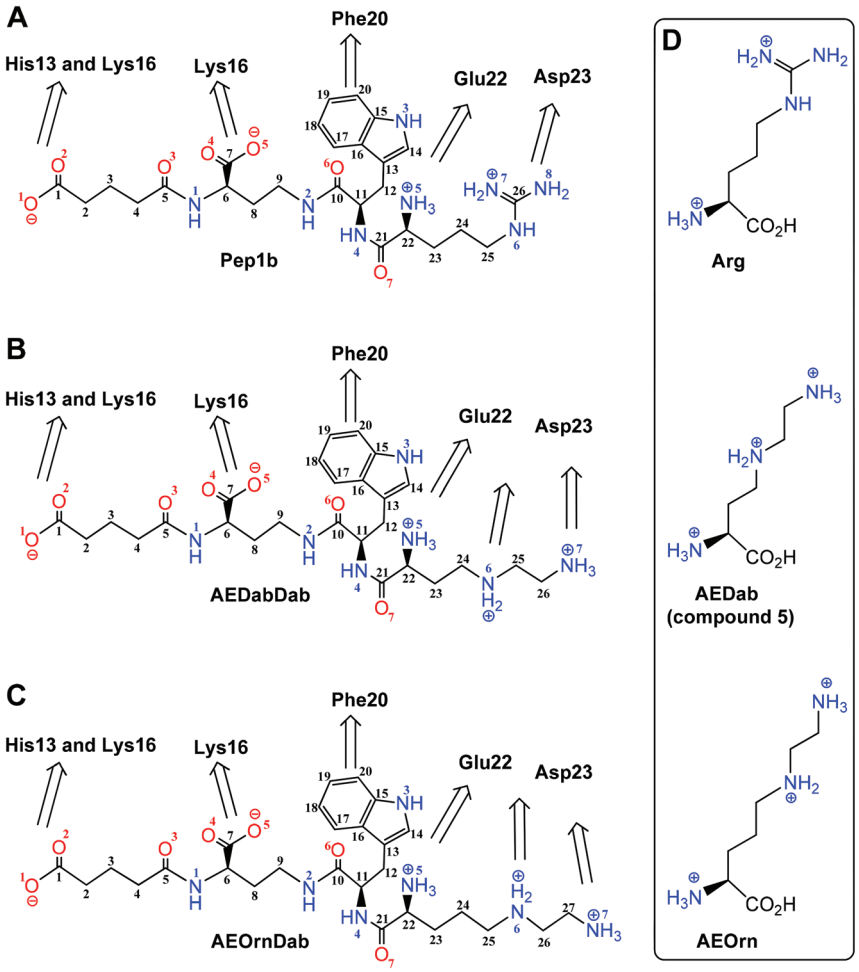

Fig. 1 Chemical structures of first-generation ligand Pep1b (A) and new ligands AEDabDab (B) and AEOrnDab (C) containing triamino acid designed to bind the α-helical form of the 13–23 region of the $A\beta_{13-26}$. The naming and numbering on ligands: carbon (black), nitrogen (blue), and oxygen (red) atoms. The naming and numbering of $A\beta_{13-26}$ residues are shown in black. Arrows indicate the interactions between $A\beta_{13-26}$ residues and different groups of the ligands. (D) Chemical structures of arginine (Arg) and triamino acids N^{γ}-(2-aminoethyl)-2,4-diaminobutanoic acid (AEDab) and N^{δ}-(2-aminoethyl)-2,5-diaminopentanoic acid (AEOrn) carrying two side-chain positive charges.

Table 1 Average αHBs count, backbone RMSD of $A\beta_{13-26}$ in the absence and presence of Pep1b, AEDabDab, and AEOrnDab, and average number of polar and non-polar contacts between $A\beta_{13-26}$ and the corresponding ligands

	Average αHBs count	Average backbone heavy atoms RMSD (Å)	Average number of polar contacts with ligand	Average number of non-polar contacts with ligand
$A\beta_{13-26}$	1.6	3.9	—	—
$A\beta_{13-26}$–Pep1b	4.6	0.8	5.9	26.8
$A\beta_{13-26}$–AEDabDab	4.8	0.9	6.3	33.6
$A\beta_{13-26}$–AEOrnDab	4.4	1.1	2.6	36.1

Synthesis of AEDab triamino acid building blocks

The Pep1b ligand was synthesized in solution using an active ester coupling approach.[20] For preparation of the new AEDabDab ligand we decided to evaluate the use of solid-phase synthesis. The AEDab building block was equipped with a benzyloxycarbonyl (Cbz) protecting group at the α-amino and at the secondary amino function of the side chain and with a *tert*-butoxycarbonyl (Boc) protection at the primary amine of the side chain. We also prepared an AEDab building block with a 9-fluorenylmethoxycarbonyl (Fmoc) protection at the primary amine of the side chain, which allows further modification of the solid supported ligand at that position for future studies.

The key step for the preparation of AEDab triamino acid building blocks was reductive alkylation of the α-amino-

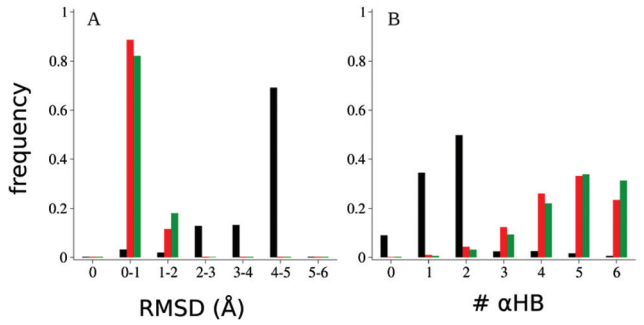

Fig. 2 Distribution of the backbone heavy atoms RMSD (A) and number of αHBs (B) of $A\beta_{13-26}$ middle region (15–24) at 360 K in $A\beta_{13-26}$ alone (black), $A\beta_{13-26}$ with Pep1b (red), and $A\beta_{13-26}$ with AEDabDab (green).

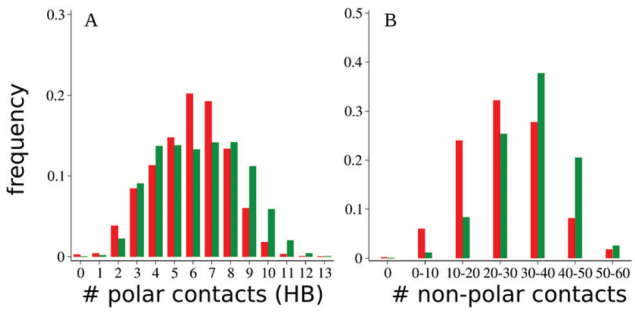

Fig. 3 Distribution of the number of polar, *i.e.*, the number of hydrogen bonds (HB), and non-polar contacts between $A\beta_{13-26}$ and Pep1b (red) and AEDabDab (green) at 360 K.

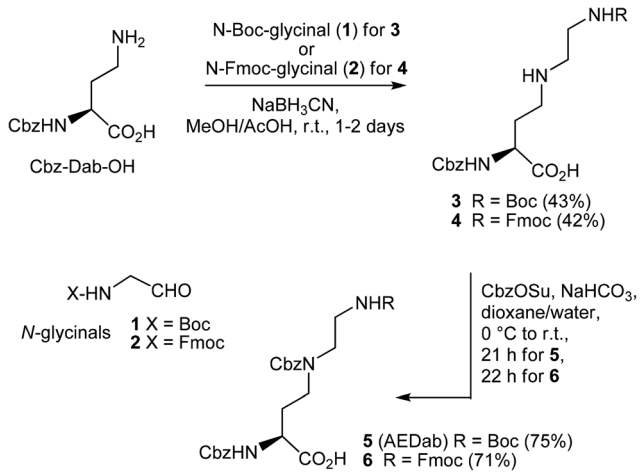

Scheme 1 Synthesis of α- and γ-*N*-Cbz-protected triamino acids (**5** and **6**) with *N*-Fmoc and *N*-Boc protected side chain.

protected diamino acid with the N-protected glycinal in the presence of the reducing agent sodium cyanoborohydride.

To avoid protection/deprotection of the carboxyl function of the amino acid we developed a strategy for the synthesis of the AEDab building blocks **5** and **6** where the carboxyl is not protected, thus saving steps. This also allowed us to directly incorporate the Fmoc protecting group on the side chain of the triamino acid **6**. α-Amino protected Cbz-Dab-OH was subjected to reductive alkylation with N-protected-glycinals **1** and **2** (Scheme 1). Due to the poor solubility of the starting material in methanol (MeOH) containing 1% acetic acid (AcOH), the reaction was first performed in a methanol–water mixture in the presence of a quaternary ammonium salt Bu_4NHSO_4 which afforded compound **3** in 29% yield. However, product yields were improved when a higher concentration of AcOH in MeOH was used. Thus the reductive alkylation of Cbz–Dab–OH in the presence of $NaBH_3CN$ afforded intermediate **3** in 43% yield in the reaction with *N*-Boc-glycinal **1** in 2.5% AcOH in MeOH, and gave product **4** (42%) in the reaction with *N*-Fmoc-glycinal[31] **2** in 5% AcOH in MeOH. Subsequent protection of secondary amino function with the Cbz protecting group afforded compounds **5** and **6**, respectively.

Preparation of the Aβ targeting ligand AEDabDab

The AEDab triamino acid building block **5** was used in the synthesis of the novel Aβ targeting ligand AEDabDab (compound **12**, Scheme 2). The assembly of the AEDabDab by solid-phase synthesis was performed using an Fmoc chemistry procedure. The synthesis started with the attachment of glutaric anhydride to the polystyrene Wang resin (0.9 mmol g^{-1}) in the presence of 4-(dimethylamino)pyridine (DMAP). The obtained resin product **7** was in a reversed coupling connected to the α-amino group of the D-amino acid H-D-Dab(Fmoc)-OMe (prepared by copper complex-mediated side chain protection[32,33] followed by thionyl chloride-mediated esterification[34]). *t*-Butyl protection could be a more obvious choice but we picked methyl protection due the better procedures for preparation. Deprotection of the Fmoc group on **8** could potentially lead to intramolecular nucleophilic reaction of the free primary amine with the methyl ester. However, no such side product arising from such a reaction was detected later in the crude **11** after cleavage from resin, which is perhaps not very surprising since the effective molarity for cyclization of flexible primary alkylamines is rather modest.[35] In the subsequent step, D-tryptophan (Fmoc-D-Trp-OH) was attached to the γ-amino function of the D-Dab residue to give **9**. After removal of the Fmoc from the D-Trp residue, coupling of the new triamino acid building block **5** to the α-amino function of the D-Trp was performed using HATU as the activating agent to give **10**. Removal of the Boc and the two Cbz protecting groups as well as cleavage from the solid support was performed by treatment of the resin with a trifluoroacetic acid–phenol–water–triisopropylsilane (TFA–phenol–H_2O–TIS) cleavage cocktail and afforded intermediate **11** in 32% overall yield for five steps. Hydrolysis of the methyl ester **11** under basic conditions resulted in the final compound **12**, which was isolated as the main product by reversed-phase HPLC.

Effect of the AEDabDab ligand on Aβ-induced reduction of gamma oscillations

We have demonstrated that small peptide-like compounds can interfere with Aβ aggregation and inhibit Aβ neurotoxicity by preventing the Aβ-induced reduction of rhythmic network

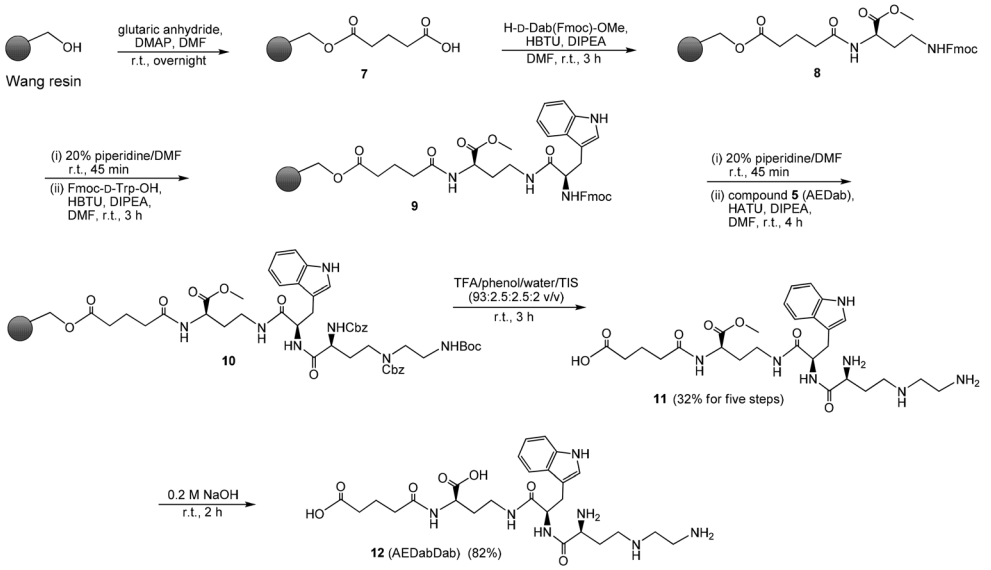

Scheme 2 Synthesis of the AEDabDab ligand using triamino acid building block 5 (AEDab).

activity in the gamma-frequency range (30–80 Hz, gamma (γ) oscillations[36,37]) in hippocampal slice preparations.[20] Gamma oscillations play an important role in higher processes in the brain, such as learning, memory and cognition, and are markedly reduced in patients diagnosed with Alzheimer's disease.[22] To study the impact of the new ligand AEDabDab on the ability to reduce Aβ neurotoxicity we tested and compared its activity with the first-generation ligand Pep1b in γ oscillation experiments.

Gamma oscillations were induced by superfusing horizontal hippocampal slices from C57BL/6 mice with 100 nM kainate. LFP recordings in area CA3 revealed control γ oscillations of 5.58 10^{-09} ± 3.98 10^{-10} V^2 power (n = 16; Fig. 4A). When slices were incubated for 15 min with 50 nM $A\beta_{1-42}$ prior to kainate superfusion the resulting γ oscillation power was significantly decreased (1.97 × 10^{-09} ± 2.98 × 10^{-10} V^2; n = 12; U = 188.0, $n1$ = 16, $n2$ = 12, p < 0.0001 two-tailed; Fig. 4B). Addition of the ligand AEDabDab to the incubation solution strongly prevented Aβ-induced decrease of γ oscillations (6.20 × 10^{-09} ± 7.38 × 10^{-10} V^2; n = 13; AEDabDab *vs.* control kainate: U = 110.0, $n1$ = 16, $n2$ = 13, p = 0.813 two-tailed; Fig. 4C and 4E). Noticeably, AEDabDab displayed a stronger inhibitory effect compared to the first-generation ligand Pep1b which showed partial prevention of the Aβ-induced reduction of γ oscillations (3.44 × 10^{-09} ± 3.15 × 10^{-10} V^2; n = 11; Pep1b *vs.* control kainate: U = 153.0, $n1$ = 16, $n2$ = 13, p = 0.0008 two-tailed; Pep1b *vs.* Aβ: U = 110.0, $n1$ = 12, $n2$ = 13, p = 0.0056 two-tailed; Fig. 4D and 4F).

Control experiments when slices were incubated only in the presence of AEDabDab or Pep1b (in the absence of Aβ) before kainate superfusion showed that neither ligand alone had any effect on kainate-induced γ oscillations ((AEDabDab, 5.39 × 10^{-09} ± 3.49 × 10^{-10} V^2; n = 8); (Pep1b, 4.38 10^{-09} ± 2.65 10^{-10} V^2; n = 8); Fig. 5). Enhancement of the effect in preventing the Aβ-induced reduction of γ oscillations in the presence of AEDab-

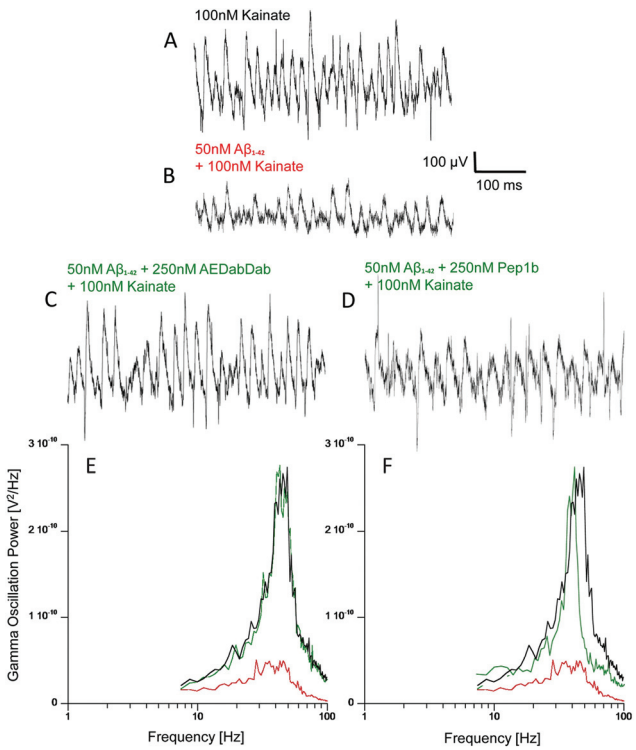

Fig. 4 Inhibitory effect of the ligand AEDabDab and the first-generation ligand Pep1b on the Aβ-induced reduction of γ oscillation in hippocampal slices. (A) Traces of kainate-induced γ oscillations in area CA3 of naïve slices. (B) Reduction of γ oscillation power after 15 min incubation with 50 nM $A\beta_{1-42}$ before kainate superfusion. (C) Traces of kainate-induced γ oscillations after incubation with 50 nM $A\beta_{1-42}$ in the presence of 250 nM AEDabDab. (D) Traces of kainate-induced γ oscillations after incubation with 50 nM $A\beta_{1-42}$ in the presence of 250 nM Pep1b. (E) Power spectra of γ oscillations in a naïve slice (black), after incubation with $A\beta_{1-42}$ alone (red) and in the presence of AEDabDab (green). (F) Power spectra of γ oscillations in a naïve slice (black), after incubation with $A\beta_{1-42}$ alone (red) and in the presence of Pep1b (green).

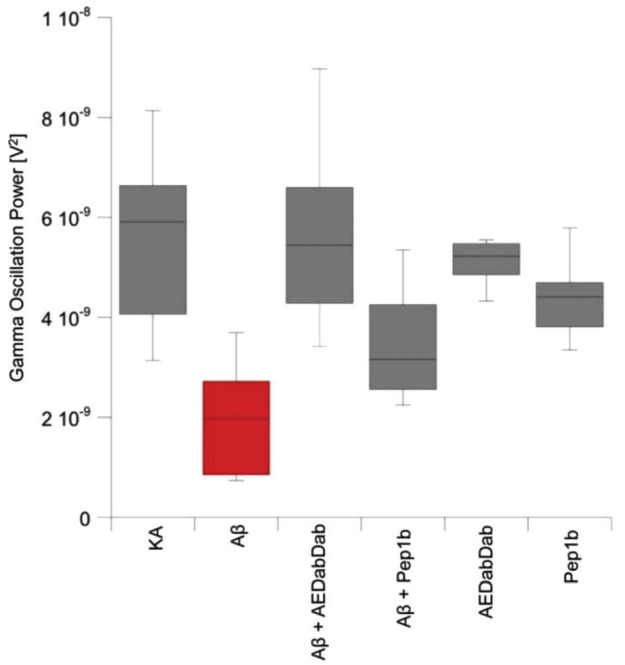

Fig. 5 Summary histogram of γ oscillation power in naïve slices (KA), $Aβ_{1–42}$ incubated slices (Aβ), $Aβ_{1–42}$ incubated slices in the presence of the ligand AEDabDab (Aβ + AEDabDab), $Aβ_{1–42}$ incubated slices in the presence of the ligand Pep1b (Aβ + Pep1b), AEDabDab-only incubated slices (AEDabDab) and Pep1b-only incubated slices (Pep1b).

Dab (Fig. 5) can be attributed to the additional stabilisation of the Aβ due to the newly incorporated triamino acid moiety.

Conclusion

In conclusion, the novel Aβ targeting ligand AEDabDab containing a new triamino acid, N^{γ}-(2-aminoethyl)-2,4-diaminobutanoic (AEDab) acid, is developed in order to improve interaction of the ligand with the helical conformation of the central part of Aβ. Molecular dynamics indicate that introduction of the AEDab triamino acid residue with an extra positive charge into an Aβ targeting ligand has a favourable effect on the Aβ–ligand interaction and enhances the ligand's ability to stabilize the α-helical conformation. We could also show by γ oscillation experiments that the replacement of the arginine moiety by a triamino acid in the new AEDabDab ligand improves prevention of Aβ neurotoxicity. The data from the modeling studies and *in vitro* γ oscillation experiments support the fact that enhancement of ligand affinity to the helical Aβ is possible through additional cationic interactions between the positively charged amino acid and negatively charged Aβ residues.

Experimental

General information

Commercially available amino acids were purchased from Bachem AG (Switzerland) and IRIS Biotech GmbH (Germany). All other chemicals and solvents (all of analytical grade) were obtained from commercial sources and used without further purification. Thin layer chromatography (TLC) was performed on Merck pre-coated silica gel 60 F254 glass-backed plates and visualized by UV and by spraying with ninhydrin solution (6 g of ninhydrin in 100 mL of ethanol). Chromatographic separations were performed on Merck G60 silica gel. Mass analysis was performed with a Micromass LCT ESI-TOF mass spectrometer using leucine enkephaline as an internal mass standard. ^{1}H NMR spectra were recorded at 400 MHz, and ^{13}C NMR spectra at 100.6 MHz using either tetramethylsilane (TMS) or the deuterated solvent as an internal standard. Chemical shifts (δ scale) are reported in ppm. Coupling constants (J values) are given in hertz (Hz). HPLC purification was performed by reversed-phase (RP) HPLC on a GraceVydac Protein & Peptide C18 preparative column (300 Å pore size, 13 μm particle size) with a linear gradient from 5% to 60% or 20% to 80% of solvent B in A (solvent A = 0.1% TFA in water; solvent B = 0.1% TFA in 90% aqueous acetonitrile) over 40 min. Chemical compounds used in intracellular and extracellular solutions were obtained from Sigma-Aldrich Sweden AB (Stockholm, Sweden), and kainic acid was obtained from Tocris. Met-$Aβ_{1–42}$ was expressed in *Escherichia coli* BL21 from synthetic genes and purified as described.[38] Monomeric $Aβ_{1–42}$ was obtained by lyophilizing concentrated $Aβ_{1–42}$ peptide, dissolving it in 7 M guanidine hydrochloride and subjecting it to a size exclusion chromatography (SEC) column.

Synthesis of amino acids

N^2-Benzyloxycarbonyl-N^4-(*N-tert*-butoxycarbonyl-2-aminoethyl)-(*S*)-2,4-diaminobutanoic acid (3). *Method A*. N^2-Benzyloxycarbonyl-L-2,4-diaminobutanoic acid (Cbz-Dab-OH, 0.5 g, 2.0 mmol) was dissolved in water (20 ml) and tetrabutylammonium hydrogensulphate (0.68 g, 2.0 mmol) was added at room temperature followed by 1.26 mL of a solution of *N-tert*-butoxycarbonylglycinal (0.35 g, 2.2 mmol) in methanol. After 30 min sodium cyanoborohydride (0.38 g, 6.0 mmol) was added portionwise over 30 min and the reaction mixture was stirred for 18 h. The solvents were removed *in vacuo* and the residue was re-dissolved in water and lyophilized. Methanol was added and the insoluble material was filtered off. The filtrate was concentrated and the product was purified by flash column chromatography using first EtOAc–MeOH–AcOH (20 : 2 : 1 v/v) and then EtOAc–MeOH–AcOH–H_2O (10 : 2 : 1 : 1 v/v) as the eluent. The collected fractions were combined, concentrated *in vacuo* and traces of AcOH were removed by co-evaporation with a toluene–methanol mixture to afford **3** (0.23 g, 29%).

Method B. To a suspension of Cbz-Dab-OH (0.5 g, 2.0 mmol) in 40 mL of anhydrous methanol containing 2.5% of AcOH *N-tert*-butoxycarbonylglycinal (0.35 g, 2.2 mmol) was added and the reaction mixture was stirred for 45 min at room temperature under a nitrogen atmosphere. Sodium cyanoborohydride (0.38 g, 6.0 mmol) was added portionwise over 30 min and the reaction mixture was kept stirring overnight. Additional portions of *N-tert*-butoxycarbonylglycinal (0.16 g, 1.0 mmol) and sodium cyanoborohydride (0.38 g, 6.0 mmol)

were added and the reaction was stirred for an additional 4 h. The solvents were removed *in vacuo* and the residue was dissolved in water, acidified with 1 M aqueous $KHSO_4$ and extracted with ethyl acetate. The organic phase was washed with brine, water, dried over Na_2SO_4, filtered and concentrated under reduced pressure. The residue was subjected to flash column chromatography using first EtOAc–MeOH–AcOH (20 : 2 : 1 v/v) and then EtOAc–MeOH–AcOH–H_2O (10 : 2 : 1 : 1 v/v) as the eluent. The collected fractions were combined, concentrated *in vacuo* and traces of AcOH were removed by co-evaporation with a toluene–methanol mixture. The product was re-dissolved in a small volume of water–acetonitrile (9 : 1) and lyophilized to give **3** (0.34 g, 43%). R_f = 0.50 (EtOAc–MeOH–AcOH–H_2O, 10 : 2 : 1 : 1 v/v). δ_H (400 MHz; DMSO-d_6) 7.37–7.25 (5 H, m), 6.88 (1 H, br t), 6.63 (1 H, br d), 4.99 (2 H, s), 3.75–3.68 (1 H, m), 3.10–3.00 (2 H, m), 2.75–2.59 (4 H, m), 1.85–1.72 (2 H, m), 1.36 (9 H, s); δ_C (100.6 MHz; DMSO-d_6) 173.8, 173.3, 155.6, 155.3, 137.3, 128.3, 127.7, 127.6, 77.7, 65.1, 54.4, 47.4, 45.5, 38.4, 31.0, 28.2; HRMS (ESI-TOF): calcd for $C_{19}H_{28}N_3O_6$ $[M - H]^-$ 394.1984, found 394.1978.

N^2-Benzyloxycarbonyl-N^4-[*N*-(9-fluorenylmethoxycarbonyl)-2-aminoethyl]-(*S*)-2,4-diaminobutanoic acid (4). Cbz-Dab-OH (0.4 g, 1.59 mmol) was suspended in 30 mL of anhydrous methanol containing 5% of AcOH. After stirring for 10 min *N*-(9-fluorenylmethoxycarbonyl)glycinal (0.53 g, 1.9 mmol) was added and the reaction mixture was stirred for 30 min at room temperature under a nitrogen atmosphere. Sodium cyanoborohydride (0.4 g, 6.34 mmol) was added portionwise over 30 min and the reaction mixture was kept stirring for 17 h. Additional portions of *N*-(9-fluorenylmethoxycarbonyl)glycinal (0.27 g, 0.95 mmol) and sodium cyanoborohydride (0.2 g, 3.17 mmol) were added and the reaction was stirred for another 24 h more. The solvents were evaporated *in vacuo*, and the residue was dissolved in ethyl acetate, and washed with water and brine. The organic layer was dried over Na_2SO_4, filtered and concentrated under reduced pressure. The residue was purified by flash column chromatography using first EtOAc–MeOH–AcOH (20 : 2 : 1 v/v) and then EtOAc–MeOH–AcOH–H_2O (10 : 2 : 1 : 1 v/v) as the eluent. The collected fractions were combined, solvents were evaporated *in vacuo* and the residue was dried by evaporation of an added toluene–methanol mixture. The product was dissolved in a small volume of water–acetonitrile (9 : 1) mixture and lyophilized to give compound **4** (0.35 g, 42%). R_f = 0.56 (EtOAc–MeOH–AcOH–H_2O, 10 : 2 : 1 : 1 v/v). δ_H (400 MHz; CD_3OD) 7.79 (2 H, d, J = 7.5 Hz), 7.64 (2 H, d, J = 7.4 Hz), 7.44–7.25 (9 H, m), 5.11–4.98 (2 H, m), 4.45–4.34 (2 H, m), 4.21 (1 H, br t), 4.13 (1 H, br t), 3.46–3.37 (2 H, m), 3.17–2.99 (4 H, m), 2.27–2.12 (1 H, m), 2.05–1.95 (1 H, m); δ_C (100.6 MHz, DMSO-d_6) δ = 173.6, 155.2, 142.6, 139.4, 137.4, 137.3, 128.9, 128.3, 127.65, 127.61, 127.3, 127.1, 121.4, 120.0, 65.05, 64.98, 63.5, 54.3, 46.7, 29.0, 28.7; HRMS (ESI-TOF): calcd for $C_{29}H_{30}N_3O_6$ $[M - H]^-$ 516.2140, found 516.2149.

N^4-(*N*-*tert*-Butoxycarbonyl-2-aminoethyl)-N^2,N^4-dibenzyloxycarbonyl-(*S*)-2,4-diaminobutanoic acid (5). To an ice-water bath chilled solution of compound **3** (0.179 g, 0.45 mmol) in 5 mL of 1,4-dioxane–water (1 : 1), $NaHCO_3$ (0.076 g, 0.91 mmol) was added. To the resulting solution *N*-(benzyloxycarbonyloxy)succinimide (0.169 g, 0.68 mmol) was added whereupon the reaction mixture was allowed to warm to ambient temperature and was stirred for 21 h. The solvents were evaporated *in vacuo* and the residue was re-dissolved in water, acidified with 1 M aqueous $KHSO_4$ and extracted with ethyl acetate. The organic layer was dried over Na_2SO_4, filtered and concentrated under reduced pressure. The residue was subjected to flash column chromatography using 0 to 6% MeOH in dichloromethane containing 0.1% AcOH as the eluent. The collected fractions with the product were concentrated *in vacuo* and traces of AcOH were removed by co-evaporation with toluene to give compound **5** (0.18 g, 75%). R_f = 0.66 (CH_2Cl_2–CH_3OH–AcOH, 9 : 1 : 0.1 v/v). δ_H (400 MHz; DMSO-d_6) 7.68–7.54 (1 H, m), 7.47–7.21 (10 H, m), 6.87 (1 H, br d), 5.17–4.92 (4 H, m), 3.98–3.85 (1 H, m), 3.61–2.94 (6 H, m), 2.07–1.87 (1 H, m), 1.86–1.67 (1 H, m), 1.35 (9 H, s); δ_C (100.6 MHz; DMSO-d_6) 173.5, 156.1, 155.6, 155.3, 137.0, 136.9, 128.3, 127.8, 127.7, 127.6, 127.2, 77.6, 66.1, 65.5, 51.8, 46.9, 46.4, 44.8, 44.3, 38.6, 38.1, 29.8, 29.1, 28.2; HRMS (ESI-TOF): calcd for $C_{27}H_{34}N_3O_8$ $[M - H]^-$ 528.2351, found 528.2341.

N^2,N^4-Dibenzyloxycarbonyl-N^4-[*N*-(9-fluorenylmethoxycarbonyl)-2-aminoethyl]-(*S*)-2,4-diaminobutanoic acid (6). Compound **4** (0.24 g, 0.46 mmol) was dissolved in 12 mL of 1,4-dioxane–water (3 : 1) and chilled in an ice-water bath. To the resulting mixture $NaHCO_3$ (0.078 g, 0.93 mmol) was added followed by the addition of *N*-(benzyloxycarbonyloxy)succinimide (0.173 g, 0.69 mmol). The reaction mixture was allowed to warm to ambient temperature and was stirred for 22 h. The solvents were reduced *in vacuo*, the residue was acidified with 1 M aqueous $KHSO_4$ and extracted with ethyl acetate. The organic phase was dried over Na_2SO_4, filtered and concentrated under reduced pressure. The product was purified by flash column chromatography using 0 to 15% MeOH in dichloromethane as the eluent (silica gel column was prepared with addition of 1% AcOH in dichloromethane) to afford **6** (0.215 g, 71%). R_f = 0.36 (CH_2Cl_2–CH_3OH, 9 : 1 v/v). δ_H (400 MHz; DMSO-d_6) 7.88 (2 H, d, J = 7.5 Hz), 7.70–7.61 (2 H, m), 7.42–7.27 (15 H, m), 7.15–7.03 (1 H, m), 5.10–4.91 (4 H, m), 4.31–4.12 (3 H, m), 3.87–3.75 (1 H, m), 3.56–2.99 (6 H, m), 2.07–1.89 (1 H, m), 1.85–1.67 (1 H, m); δ_C (100.6 MHz; DMSO-d_6) 174.3, 156.2, 155.8, 155.4, 155.2, 143.9, 140.7, 137.1, 137.0, 128.9, 128.31, 128.30, 127.71, 127.66, 127.60, 127.3, 127.2, 127.0, 125.2, 120.1, 120.0, 66.0, 65.4, 65.2, 52.9, 46.7, 46.0, 44.8, 44.3, 38.4, 30.9, 30.2 ppm. HRMS (ESI-TOF): calcd for $C_{37}H_{36}N_3O_8$ $[M - H]^-$ 650.2508; found 650.2506.

Preparation of the Aβ targeting ligand

N^4-(2-Aminoethyl)-L-Dab-D-Trp-N^4-D-Dab-OMe-N^2-glutarate (11). The Wang resin (0.29 g, 0.26 mmol, 0.9 mmol g^{-1}, 100–200 mesh) was swollen in DMF (2 mL) for 30 min. Glutaric anhydride (0.15 g, 1.32 mmol) and DMAP (0.032 g, 0.26 mmol) in DMF (1 mL) were added and the reaction was kept overnight at ambient temperature under a nitrogen flow. The resin product was filtered, washed with DMF, methanol

and dichloromethane, and dried *in vacuo*. Assembly of the sequence was performed manually using the Fmoc protocol. For the reverse coupling of amino acid H-D-Dab(Fmoc)-OMe (0.37 g, 1.04 mmol) and for the amino acid Fmoc-D-Trp-OH (0.44 g, 1.04 mmol), HBTU (0.39 g, 1.04 mmol) and DIPEA (0.27 mL, 1.56 mmol) in DMF (2 mL) were used as activating agents. The carboxylic function of intermediate **7** and Fmoc-D-Trp-OH was pre-activated with HBTU prior to the addition of the corresponding amino compounds. Coupling of compound **5** (0.55 g, 1.04 mmol) was achieved in the presence of HATU (0.39 g, 1.04 mmol) and DIPEA (0.27 mL, 1.56 mmol). Coupling reactions were performed for 3 h except for coupling of **5**, which was kept for 4 h. Deprotection of the *N*-Fmoc group was achieved by treatment with 20% piperidine in DMF for 30 min and additional 15 min using a fresh piperidine–DMF mixture. After each coupling reaction and Fmoc-deprotection the resin was washed sequentially with DMF, methanol, dichloromethane and again with DMF. Deprotection of the product and cleavage from the solid support (0.062 g of the resin) was achieved by the treatment with TFA–phenol–H_2O–TIS (93 : 2.5 : 2.5 : 2 v/v, 10 mL g^{-1} of polymer) for 3 h at room temperature. The mixture was filtered and volatiles were evaporated under reduced pressure. The crude product was precipitated with cold diethyl ether, centrifuged and washed with an additional portion of diethyl ether. The residue was redissolved in water and lyophilized to give crude intermediate **11** (0.029 g). A sample (5 mg) of this intermediate was purified by RP-HPLC for analytical purposes to give compound **11** (1.6 mg, 32% for five steps, recalculated overall yield of solid phase synthesis). RP-HPLC conditions: linear gradient elution from 20% to 80% of solvent B (solvent A = 0.1% TFA in water; solvent B = 0.1% TFA in 90% aqueous acetonitrile) over 40 min, t_R 16.12 min. δ_H (400 MHz; D_2O) 7.63 (1 H, d, J = 7.9 Hz,), 7.46 (1 H, d, J = 8.1 Hz), 7.25–7.09 (3 H, m), 4.65 (1 H, t, J = 8.0 Hz), 4.20 (1 H, dd, J = 4.9, 9.4 Hz), 3.71 (3 H, s), 3.40 (1 H, dd, J = 4.4, 9.8 Hz), 3.28–3.08 (4 H, m), 2.97–2.76 (4 H, m), 2.62–2.48 (4 H, m), 2.46–2.38 (1 H, m), 2.33–2.23 (1 H, m), 1.71–1.59 (1 H, m), 1.57–1.46 (1 H, m), 1.19–0.84 (4 H, m); HRMS (ESI-TOF): calcd for $C_{27}H_{40}N_7O_7$ $[M - H]^-$ 574.2995, found 574.2988.

***N*^{4}-(2-Aminoethyl)-L-Dab-D-Trp-*N*^{4}-D-Dab-*N*^{2}-glutarate (12).** A solution of compound **11** (0.75 mg, 1.3 μmol) in deionized water (0.25 mL) was treated with 0.4 M NaOH (0.25 mL) for 2 h at ambient temperature. After completion of the reaction 0.5 M aqueous TFA (0.3 mL) was added and the crude product was purified by RP-HPLC with a linear gradient elution from 5% to 60% of solvent B (solvent A = 0.1% TFA in water; solvent B = 0.1% TFA in 90% aqueous acetonitrile) over 40 min, t_R 21.98 min. The acetonitrile was removed from the collected fractions *in vacuo* and the aqueous solution was then lyophilized to afford compound **12** (0.6 mg, 82%). δ_H (400 MHz; D_2O) 7.70 (1 H, d, J = 7.9 Hz,), 7.54 (1 H, d, J = 8.1 Hz), 7.33–7.17 (3 H, m), 4.98–4.60 (1 H, m, D_2O residual peak), 4.25 (1 H, dd, J = 4.7, 9.1 Hz), 3.48 (1 H, dd, J = 4.4, 9.6 Hz), 3.35–3.15 (4 H, m), 3.06–2.83 (4 H, m), 2.71–2.56 (4 H, m), 2.54–2.46 (1 H, m), 2.42–2.32 (1 H, m), 1.81–1.69 (1 H, m), 1.67–1.55 (1 H, m), 1.28–0.96 (4 H, m); HRMS (ESI-TOF): calcd for $C_{26}H_{38}N_7O_7$ $[M - H]^-$ 560.2838, found 560.2826.

Molecular modeling

The initial model structure of $A\beta_{13-26}$ was built in an α-helical conformation as in our previous simulation studies.[24,25] Since $A\beta_{13-26}$ is a fragment of the full peptide, the N- and C-termini have been made neutral by capping with N-terminal acetyl and C-terminal amide groups respectively, mimicking the uncharged amide linkage on both ends of $A\beta_{13-26}$ in the full length peptide. The peptides were built with the ionizable residues in their charged states, where basic residues (H13, H14 and K16) are protonated and acidic residues (E22 and D23) are deprotonated. Thus, the total charge on $A\beta_{13-26}$ is +1e.

The structures of $A\beta_{13-26}$ with Pep1b ($A\beta_{13-26}$–Pep1b), AEDabDab ($A\beta_{13-26}$–AEDabDab) and AEOrnDab ($A\beta_{13-26}$–AEOrnDab) were built using the Insight II program.[25,39] The complexes were designed to obtain interactions with the amino acids His-13, Lys-16, Phe-20, Glu-22 and Asp-23 as described above (Fig. 1) and with all basic amino acids in their protonated state and acidic amino acids in their deprotonated state.

Simulations are performed at 360 K for $A\beta_{13-26}$ alone[25] and with ligands (Pep1b,[25] AEDabDab, and AEOrnDab). The temperature in each simulation was maintained by coupling all atoms to a Langevin heat bath with frictional coefficient β = 2 ps^{-1}.[40] All simulations and analyses were carried out using the CHARMM[41,42] version c36a6 with the CHARMM22/CMAP all-hydrogen force field[43,44] using the implicit solvent (IS) model GBMV II.[29] The ligands are peptidomimetic and are designed using amino acid moieties, with force field parameters transferred from analogous groups in the protein force field, and therefore ligands can be used without any problem with GBMV II. The SHAKE algorithm[45] was used to fix the length of the covalent bonds involving hydrogen atoms, allowing an integration time step of 2 fs to be used in the integration of Newton's equations. The simulation parameters specific to GBMV II are similar to those used in an earlier IS simulation study (see Table 4 of Juneja *et al.*[25]). All calculations were performed on a GNU/Linux PC cluster with 64 bit Intel Xeon and AMD processors. Before the simulations, structures of respective models ($A\beta_{13-26}$ alone and $A\beta_{13-26}$ with ligands) were optimized by 2000 steps of steepest descent followed by 4000 steps of the adopted basis Newton–Raphson. The system was heated up to the target temperature of 360 K gradually for 20 ps employing velocity rescaling. The system was then shifted to the Langevin heat bath of the respective temperature and equilibrated for 30 ps. After equilibration, production runs of 100 ns were carried out with coordinates saved every 1 ps.

Every snapshot (1 ps) of the production run (100 ns) was analyzed. To examine the effect of ligands on the structural changes in $A\beta_{13-26}$, the root-mean-square deviation (RMSD) and the number of α-helical backbone hydrogen bonds (αHBs) of the residues 15–24 of $A\beta_{13-26}$ were calculated in the presence of ligands employing similar criteria from our previous

study.[25] The root-mean-square deviation (RMSD) was computed for the middle region (15–24) of $A\beta_{13-26}$ thus avoiding large fluctuations originating from mobile N- and C-termini. The reported backbone heavy atom RMSD was calculated against the initial energy-minimized coordinates along the MD simulation. The αHBs were defined using the criterion acceptor–hydrogen distance <2.4 Å.[46] Polar contacts were determined by counting the number of hydrogen bonds between $A\beta_{13-26}$ and ligands. Non-polar interactions were determined considering C–C and C–N contacts using distance <5.0 Å, extracted from vdW radii of carbon, nitrogen and hydrogen, and C–H and N–H covalent bond-lengths. Ligands are designed to have non-polar interactions between backbone and side chain carbon atoms (excluding backbone carbonyl carbons) of $A\beta_{13-26}$ middle non-polar residues ($L_{17}VFFA_{21}$) and heavy atoms of the indole moiety (C_{13}–C_{20} and N_3) of ligands.

Animals

Experiments were carried out in accordance with an ethical permit granted by Norra Stockholms Djurförsöksetiska Nämnd to AF (N45/13). C57BL/6 mice of either sex (postnatal days 14–23, supplied from Charles River, Germany) were used in all experiments. The animals were deeply anaesthetized using isofluorane before being sacrificed by decapitation.

Tissue preparation

The brain was dissected out and placed in ice-cold ACSF (artificial cerebrospinal fluid) modified for dissection. This solution contained (in mM): 80 NaCl, 24 $NaHCO_3$, 25 glucose, 1.25 NaH_2PO_4, 1 ascorbic acid, 3 Na pyruvate, 2.5 KCl, 4 $MgCl_2$, 0.5 $CaCl_2$, 75 sucrose. Horizontal sections (350 μm thick) of the ventral hippocampi of both hemispheres were prepared using a Leica VT1200S vibratome (Microsystems, Stockholm, Sweden). Immediately after slicing sections were transferred to a submerged incubation chamber containing standard ACSF (in mM): 124 NaCl, 30 $NaHCO_3$, 10 glucose, 1.25 NaH_2PO_4, 3.5 KCl, 1.5 $MgCl_2$, 1.5 $CaCl_2$. The chamber was held at 34 °C for at least 20 minutes after dissection. It was subsequently allowed to cool to room temperature (19–22 °C) for a minimum of 40 minutes. Peptides were added to the incubation solution 15 minutes before transferring slices to the interface-style recording chamber. While incubating, slices were continuously supplied with carbogen gas (5% CO_2, 95% O_2) bubbled into the ACSF.

Electrophysiology

Recordings were carried out in the hippocampal area CA3 with borosilicate glass microelectrodes, pulled to a resistance of 3–7 MΩ. Local field potentials (LFP) were recorded at 34 °C using microelectrodes filled with ACSF placed in stratum pyramidale. LFP oscillations were elicited by applying kainic acid (100 nM) to the extracellular bath. The oscillations were allowed to stabilize for 20 minutes before any recordings were carried out. LFP recordings were performed using a 4 channel amplifier/signal conditioner M102-amplifier (Electronics Lab, Faculty of Mathematics and Natural Sciences, University of Cologne, Cologne, Germany). The signals were sampled at 10 kHz, conditioned using a Hum Bug 50 Hz noise eliminator (Quest Scientific, North Vancouver, BC, Canada), software low-pass filtered at 1 kHz, digitized and stored using the Digidata 1322A and the Clampex 9.6 software (Molecular devices, CA, USA). Power spectral density plots (from 60 s long LFP recordings) were calculated in averaged Fourier-segments of 8192 points using Axograph X (Kagi, Berkeley, CA , USA). Oscillation power was calculated by integrating the power spectral density between 20 and 80 Hz. Data are reported as means ± standard errors of the means in the text and as median and upper/lower quartile in the figure box plots. For statistical analysis the Mann–Whitney *U*-test was used.

Acknowledgements

This work was supported by the Swedish Research Council, the Swedish Alzheimer Foundation, Eva och Oscar Ahréns Stiftelse, a KID PhD studentship grant (FRK), the Swedish Medical Association, the Swedish Brain Foundation and the Strategic Program in Neurosciences at the Karolinska Institute.

References

1 M. D. Benson, S. James, K. Scott, J. J. Liepnieks and B. Kluve-Beckerman, *Kidney Int.*, 2008, **74**, 218.
2 P. Westermark, M. D. Benson, J. N. Buxbaum, A. S. Cohen, B. Frangione, S. Ikeda, C. L. Masters, G. Merlini, M. J. Saraiva and J. D. Sipe, *Amyloid*, 2007, **14**, 179.
3 D. J. Selkoe, *Physiol. Rev.*, 2001, **81**, 741.
4 M. P. Mattson, *Physiol. Rev.*, 1997, **77**, 1081.
5 W. P. Esler and M. S. Wolfe, *Science*, 2001, **293**, 1449.
6 J. A. Hardy and G. A. Higgins, *Science*, 1992, **256**, 184.
7 M. Goedert and M. G. Spillantini, *Science*, 2006, **314**, 777.
8 J. Hardy and D. J. Selkoe, *Science*, 2002, **297**, 353.
9 D. M. Walsh, I. Klyubin, J. V. Fadeeva, W. K. Cullen, R. Anwyl, M. S. Wolfe, M. J. Rowan and D. J. Selkoe, *Nature*, 2002, **416**, 535.
10 S. Lesne, M. T. Koh, L. Kotilinek, R. Kayed, C. G. Glabe, A. Yang, M. Gallagher and K. H. Ashe, *Nature*, 2006, **440**, 352.
11 Y. Kallberg, M. Gustafsson, B. Persson, J. Thyberg and J. Johansson, *J. Biol. Chem.*, 2001, **276**, 12945.
12 L. O. Tjernberg, J. Naslund, F. Lindqvist, J. Johansson, A. R. Karlstrom, J. Thyberg, L. Terenius and C. Nordstedt, *J. Biol. Chem.*, 1996, **271**, 8545.
13 R. Liu, C. McAllister, Y. Lyubchenko and M. R. Sierks, *J. Neurosci. Res.*, 2004, **75**, 162.
14 A. T. Petkova, Y. Ishii, J. J. Balbach, O. N. Antzutkin, R. D. Leapman, F. Delaglio and R. Tycko, *Proc. Natl. Acad. Sci. U. S. A.*, 2002, **99**, 16742.
15 J. X. Lu, W. Qiang, W. M. Yau, C. D. Schwieters, S. C. Meredith and R. Tycko, *Cell*, 2013, **154**, 1257.

16 K. Janek, S. Rothemund, K. Gast, M. Beyermann, J. Zipper, H. Fabian, M. Bienert and E. Krause, *Biochemistry*, 2001, **40**, 5457.
17 E. D. Roberson and L. Mucke, *Science*, 2006, **314**, 781.
18 J. M. Mason, N. Kokkoni, K. Stott and A. J. Doig, *Curr. Opin. Struct. Biol.*, 2003, **13**, 526.
19 F. E. Cohen and J. W. Kelly, *Nature*, 2003, **426**, 905.
20 C. Nerelius, A. Sandegren, H. Sargsyan, R. Raunak, H. Leijonmarck, U. Chatterjee, A. Fisahn, S. Imarisio, D. A. Lomas, D. C. Crowther, R. Stromberg and J. Johansson, *Proc. Natl. Acad. Sci. U. S. A.*, 2009, **106**, 9191.
21 D. C. Crowther, K. J. Kinghorn, E. Miranda, R. Page, J. A. Curry, F. A. Duthie, D. C. Gubb and D. A. Lomas, *Neuroscience*, 2005, **132**, 123.
22 U. Ribary, A. A. Ioannides, K. D. Singh, R. Hasson, J. P. Bolton, F. Lado, A. Mogilner and R. Llinas, *Proc. Natl. Acad. Sci. U. S. A.*, 1991, **88**, 11037.
23 M. Ito, J. Johansson, R. Stromberg and L. Nilsson, *PLoS One*, 2011, **6**, e17587.
24 M. Ito, J. Johansson, R. Stromberg and L. Nilsson, *PLoS One*, 2012, **7**, e30510.
25 A. Juneja, M. Ito and L. Nilsson, *J. Chem. Theory Comput.*, 2013, **9**, 834.
26 D. Honcharenko, P. P. Bose, J. Johansson and R. Stromberg, in *Proceedings of the Twenty-Second American Peptide Symposium, American Peptide Society*, ed. M. Lebl, Prompt Scientific Publishing, San Diego, 2011, p. 370.
27 S. R. Chhabra, A. Mahajan and W. C. Chan, *Tetrahedron Lett.*, 1999, **40**, 4905.
28 S. R. Chhabra, A. Mahajan and W. C. Chan, *J. Org. Chem.*, 2002, **67**, 4017.
29 M. S. Lee, M. Feig, F. R. Salsbury Jr. and C. L. Brooks 3rd, *J. Comput. Chem.*, 2003, **24**, 1348.
30 M. S. Lee, F. R. Salsbury and C. L. Brooks, *J. Chem. Phys.*, 2002, **116**, 10606.
31 N. Matsumori, R. Masuda and M. Murata, *Chem. Biodiversity*, 2004, **1**, 346.
32 F. Albericio, E. Nicolas, J. Rizo, M. Ruiz-Gayo, E. Pedroso and E. Giralt, *Synthesis*, 1990, 119.
33 S. Nowshuddin and A. R. Reddy, *Tetrahedron Lett.*, 2006, **47**, 5159.
34 T. T. Charvat, D. J. Lee, W. E. Robinson and A. R. Chamberlin, *Bioorg. Med. Chem.*, 2006, **14**, 4552.
35 A. J. Kirby, *Adv. Phys. Org. Chem.*, 1980, **17**, 183–278.
36 A. Fisahn, *J. Physiol.*, 2005, **562**, 65.
37 A. Fisahn, F. G. Pike, E. H. Buhl and O. Paulsen, *Nature*, 1998, **394**, 186.
38 D. M. Walsh, E. Thulin, A. M. Minogue, N. Gustavsson, E. Pang, D. B. Teplow and S. Linse, *FEBS J.*, 2009, **276**, 1266.
39 Insight II, 2000, Available:http://www.accelrys.com.
40 R. J. Loncharich, B. R. Brooks and R. W. Pastor, *Biopolymers*, 1992, **32**, 523.
41 B. R. Brooks, R. E. Bruccoleri, B. D. Olafson, D. J. States, S. Swaminathan and M. Karplus, *J. Comput. Chem.*, 1983, **4**, 187.
42 B. R. Brooks, C. L. Brooks, A. D. Mackerell, L. Nilsson, R. J. Petrella, B. Roux, Y. Won, G. Archontis, C. Bartels, S. Boresch, A. Caflisch, L. Caves, Q. Cui, A. R. Dinner, M. Feig, S. Fischer, J. Gao, M. Hodoscek, W. Im, K. Kuczera, T. Lazaridis, J. Ma, V. Ovchinnikov, E. Paci, R. W. Pastor, C. B. Post, J. Z. Pu, M. Schaefer, B. Tidor, R. M. Venable, H. L. Woodcock, X. Wu, W. Yang, D. M. York and M. Karplus, *J. Comput. Chem.*, 2009, **30**, 1545.
43 A. D. MacKerell, D. Bashford, M. Bellott, R. L. Dunbrack, J. D. Evanseck, M. J. Field, S. Fischer, J. Gao, H. Guo, S. Ha, D. Joseph-McCarthy, L. Kuchnir, K. Kuczera, F. T. K. Lau, C. Mattos, S. Michnick, T. Ngo, D. T. Nguyen, B. Prodhom, W. E. Reiher, B. Roux, M. Schlenkrich, J. C. Smith, R. Stote, J. Straub, M. Watanabe, J. Wiorkiewicz-Kuczera, D. Yin and M. Karplus, *J. Phys. Chem. B*, 1998, **102**, 3586.
44 A. D. MacKerell, M. Feig and C. L. Brooks, *J. Am. Chem. Soc.*, 2004, **126**, 698.
45 J. P. Ryckaert, G. Ciccotti and H. J. C. Berendsen, *J. Comput. Phys.*, 1977, **23**, 327.
46 H. De Loof, L. Nilsson and R. Rigler, *J. Am. Chem. Soc.*, 1992, **114**, 4028.